JOURNAL OF GEOPHYSICAL RESEARCH, VOL. 100, NO. B3, PAGES 3829–3839, MARCH 10, 1995

Constraints on mantle ^{3}He fluxes and deep-sea circulation from an oceanic general circulation model

K.A. Farley[1]

Lamont-Doherty Earth Observatory of Columbia University, Palisades, New York

E. Maier-Reimer

Max-Planck-Institut für Meteorologie, Hamburg, Germany

P. Schlosser and W.S. Broecker

Lamont-Doherty Earth Observatory of Columbia University, Palisades, New York

Abstract. We have simulated the steady-state distribution of helium in the deep sea to investigate the magnitude and spatial and temporal variability of mantle degassing and to characterize deep-sea circulation and ventilation. The simulation was produced by linking a simple source function for helium injected at mid-ocean ridges with an oceanic general circulation model (GCM). By assuming that the flux of mantle helium is linearly proportional to the seafloor spreading rate and by using previous estimates for the total flux of mantle helium into the oceans, the GCM yields an oceanic ^{3}He distribution which is in qualitative agreement with observations both in overall magnitude and in general distribution. This provides new evidence that the flux of mantle ^{3}He into the oceans is about 1000 mol/yr and that mid-ocean ridges are the dominant source of mantle helium. Although the match with observations is good in the Pacific and Indian Oceans, the simulated ^{3}He anomalies throughout the Atlantic Ocean are much higher than has been measured. Because the GCM is thought to reproduce Atlantic circulation reasonably well, this discrepancy suggests an error in the helium source function. Either helium injection is not a linear function of seafloor emplacement rate, or eruption and concomitant degassing are highly episodic at the slow spreading rates characteristic of the Mid-Atlantic Ridge (MAR). The latter explanation would imply minimal volcanic activity along the entire length of the MAR over the last few centuries. In addition to constraints on the degassing flux, our work provides information on the transport and ventilation of deep ocean waters and constrains the degree to which current GCMs can reproduce deep-water circulation patterns. While the results generally support the GCM's abyssal circulation, our simulation reveals regions of overly-intense lateral diffusion and upwelling in the model, particularly in the equatorial Pacific. Similarly, there appears to be insufficient production of He-ventilated bottom waters in the model Antarctic. These observations suggest that further refinement of the GCM abyssal circulation is required.

Introduction

The injection of mantle helium into the deep sea can be used both to constrain the degassing of volatiles from the Earth's interior and to trace abyssal circulation. If the circulation of the oceans were well known, then the history of mantle degassing integrated over the last millennium could be retrieved from the observed helium distribution. Alternatively, if the degassing flux were well known, deep-sea circulation could be established. In reality, both mantle degassing and oceanic circulation are the subjects of considerable uncertainty. Here we present the first attempt to simulate the global oceanic helium distribution in an effort to provide additional constraints on these disparate problems.

[1]Now at Division of Geological and Planetary Sciences, California Institute of Technology, Pasadena.

Paper number 94JB02913.
0148-0227/95/94JB-02913$05.00

Mantle helium, highly enriched in the rare isotope ^{3}He, is transferred to the oceans via hydrothermal fluids associated with seafloor volcanism [*Clarke et al.*, 1969]. *Craig et al.* [1975] showed that the resulting oceanic ^{3}He inventory carries a unique record of the rate of mantle degassing. By assuming an average oceanic ^{3}He abundance and a mean bottom-water upwelling rate, these authors estimated that the release of ^{3}He from the mantle amounts to 4 ± 1 atoms/cm^2/s (~1000 ± 250 mol/yr). This value remains the best estimate of this important quantity and has been extensively used in calculations of the mantle fluxes of a wide range of chemical species. Unfortunately the estimate is highly uncertain (the ±25% figure being "minimal and optimistic") because neither the average oceanic ^{3}He abundance nor the mean upwelling rate is known. A general circulation model, using a more sophisticated treatment of oceanographic circulation, provides an additional opportunity to test this estimate. In addition, it may allow characterization of the spatial and temporal variations of the flux.

Simulation of the oceanic ^{3}He distribution can also provide insights into abyssal circulation. After hydrothermal fluids achieve neutral buoyancy, they are advected in the prevailing

currents, yielding "helium plumes" which extend for thousands of kilometers across the ocean basins [*Clarke et al.*, 1969; *Lupton and Craig*, 1981]. The conservative chemistry and high signal-to-noise ratio of these plumes makes them extraordinary tracers of deep-water flow. Transient tracers such as bomb radiocarbon, tritium, and chlorofluorocarbons are widely used indicators of circulation [e.g., *Sarmiento and Bryan*, 1982; *Weiss et al.*, 1985; *Broecker et al.*, 1985; *Schlosser et al.*, 1991a]. However, these tracers were only recently released to the environment, and hence they have penetrated only the surface ocean and the youngest of deep waters. As a consequence, deep water circulation studies must rely on alternative natural tracers such as cosmogenic ^{39}Ar and ^{14}C and mantle-derived ^{3}He. Too little is yet known of the ^{39}Ar distribution to be of great use, but several attempts have been made to interpret the global abyssal ^{14}C field [e.g., *Fiadero*, 1982; *Toggweiler et al.*, 1989]. For constraining oceanic circulation the helium modeling undertaken here is a useful complement to the ^{14}C work because the two tracers enter deep waters by completely different routes (^{14}C from surface waters and helium from middepth injection) and hence potentially provide different information.

In this paper we develop a source function for the release of helium to the deep sea and apply it to an oceanic GCM. The simulated ^{3}He distribution is then compared with measured values, and the observed discrepancies are related to characteristics of the helium flux or abyssal circulation.

Sources of Oceanic Helium

Mantle helium has a very distinctive isotopic signature: it is highly enriched in ^{3}He relative to ^{4}He compared with atmospheric and crustal helium. While ^{3}He concentrations alone could suffice as an oceanographic tracer, for analytical reasons it is the ^{3}He/^{4}He ratio of seawater samples which is commonly reported. Therefore the oceanic sources of both ^{3}He and ^{4}He must be specified in order to simulate a helium distribution which can be compared with observations.

Oceanic helium is predominantly of atmospheric origin. Seawater in contact with the atmosphere equilibrates with about 4×10^{-8} cm^3 STP He/g, which as a result of the differential solubility of the two isotopes has a slightly lower ^{3}He/^{4}He ratio than the atmosphere (δ^3He_{sw} = -1.8%, where δ^3He (%) = $100(R_{sw}/R_{air} - 1)$ and R=^{3}He/^{4}He [*Benson and Krause*, 1980]). In addition, air helium (δ^3He=0) is introduced directly into the ocean by mechanical process such as bubble injection [*Craig and Lupton*, 1981] and the melting of glacial ice [*Schlosser*, 1986]. This leads to a slight He supersaturation (the global average He supersaturation, Δ^4He, is roughly 5% [*Craig and Weiss*, 1971]). Superimposed on this steady-state and presumably homogeneous atmospheric helium background are several terrestrial and anthropogenic helium components.

Radiogenic ^{3}He is produced by the decay of tritium with a half-life of 12.43 years. The low natural abundance and short half-life of this radionuclide preclude significant tritiogenic ^{3}He in most of the deep sea. The large pulse of bomb tritium emitted in the 1960s has thus far penetrated only into deep waters of the northern Atlantic [*Jenkins and Clarke*, 1976] and, to a much lesser extent, around Antarctica. In this simulation the tritiogenic helium component has been ignored; this assumption is valid except in these restricted regions.

Compared with the atmospheric and mantle components, radiodecay of uranium-series nuclides in sediments, the oceanic crust, and in the water column is probably a negligible oceanic helium source and has been ignored. However, in certain enclosed basins with slow ventilation and little or no injection of mantle helium (e.g., Baffin Bay [*Top et al.*, 1980] and the Mediterranean [*Roether et al.*, 1992] and Black Seas [*Top and Clarke*, 1983]), this component may be important (we address this possibility below).

Mantle-derived helium is injected into the ocean by contact between seawater and recently emplaced seafloor lavas and has been detected in seawater in all active tectonic settings: mid-ocean ridges [*Craig et al.* 1975; *Jenkins et al.*, 1980; *Lupton and Craig*, 1981; *Top et al.*, 1987; *Lupton et al.*, 1989; *Jean-Baptiste et al.*, 1990; *Jamous et al.*, 1992], back-arc basins [*Schlosser et al.*, 1988], hotspots [*Gamo et al.*, 1987], and arc environments [*Belviso et al.*, 1987]. *Torgerson* [1989] has compiled estimates which indicate that the mid-ocean ridge flux is by far the most important source of mantle helium to the ocean; the second largest source contributes at most an additional 20%. In contrast, on the basis of a mantle mass transport model, *Kellogg and Wasserburg* [1990] have argued that plumes dominate the flux of mantle ^{3}He to the atmosphere. However, this suggestion is not borne out by observations which show the largest concentrations of mantle helium centered over ridges [e.g., *Lupton and Craig*, 1981] rather than over active hotspot seamounts, such as Loihi [*Gamo et al.*, 1987]. If the mass transport model is accurate, this discrepancy suggests that plumes degas mostly subaerially or perhaps episodically. For the present first-order model we have adopted the simple assumption that all helium sources other than mid-ocean ridges (and the atmosphere) can be ignored.

The GCM simulation requires specification of the latitude, longitude, depth, and magnitude of the global ridge helium source. Because helium is very efficiently extracted from fresh basalts by hydrothermal circulation [*Dymond and Hogan*, 1978], the helium flux should be directly proportional to the rate of basalt emplacement. The thickness of the oceanic crust is nearly constant throughout the ridge system [*Bown and White*, 1994], so a linear relationship between local seafloor spreading rate and helium flux should exist. Hydrothermal vents are confined to the axes of active spreading centers, and the locations of these axes are defined by seismicity and magnetic lineations. For simplicity we have assumed that hydrothermal venting is continuously distributed (i.e., it is a line source rather than a series of discrete point sources). This assumption is justified by the following considerations.

Numerous *ALVIN* studies have revealed that hydrothermal venting is localized in intense "fields" scattered along the ridge crests, probably at sites of recent magmatism. For the present purposes an important question is over what length scale the vent fields recur: is the scale short or long compared with the size of the GCM grid? Based on a detailed study of the distribution of vent sites on the Juan de Fuca Ridge, *Baker and Hammond* [1992] calculated a probability between 5 and 50% that any given portion of oceanic ridge is actively venting. The lowest probability pertains to slow spreading regimes like the Mid-Atlantic Ridge (MAR), whereas the highest rates apply to the fast spreading East Pacific Rise (EPR). Based on their identification of six major vent fields in the 360 km ridge segment studied, the recurrence interval on the Juan de Fuca Ridge is roughly 60 km. Scaling the recurrence length to the venting probability suggests that over the global ridge system the distances between vent sites should range from about 20 to 240 km. Thus in the ~400 km square grid boxes of the Hamburg GCM (see below), there are likely to be several simultaneously

operating vent sites even at the lowest spreading rates. Their exact distribution along the ridge axis is therefore not of great concern. It should be stressed that this is an assumption based on limited observations of ridges and if incorrect may lead to an "overly-smooth" simulated helium distribution.

Although hydrothermal fluids are injected at a variety of temperatures, the bulk of the plumes rise about 300 meters above the injection site before achieving neutral buoyancy [*Lupton et al.*, 1985]. Thus we have assumed that helium is introduced 300 m above the local ridge axis.

The global flux of mantle ^{3}He to the oceans is approximately 1000 mol/yr [*Craig et al*, 1975] which we assume is completely produced by mid-ocean ridge basalt (MORB) emplacement. MORB crust is produced at the rate of approximately 3.0×10^{10} cm^2/yr [*Parsons*, 1981], so the best estimate for the flux of mantle ^{3}He from the ridges is 33 nmol per cm of ridge length per cm/yr of spreading. Note that any error in the absolute flux used in the GCM will be propagated only to the magnitude of the modeled ^{3}He anomalies and not to their general distribution. Because global spreading rates have been modeled [*Minster and Jordan*, 1978; *DeMets et al.*, 1990], a continuous function for the helium flux along the entire global ridge system can be constructed (Figure 1).

Modeling the Steady State ^{3}He Distribution

The Hamburg Large-Scale Geostrophic ocean circulation model has been described in detail elsewhere [*Maier-Reimer et al.*, 1993; *Maier-Reimer*, 1993]. The model has an effective horizontal resolution of 3.5° and consists of 15 vertical levels (in deep water, these are 1, 2, 3, 4, and 5 km). Circulation is driven by a prescribed wind stress field and the observed surface layer salinity field. Smoothed, realistic bathymetry is included. Mantle helium is assumed to be a completely passive tracer (i.e., the flux of hydrothermal heat is ignored). The only sink for oceanic helium is loss to the atmosphere; oceanic degassing is suppressed when sea-ice cover exists. The ^{3}He source function is defined according to the following rules:

1. ^{3}He is injected only on the mid-ocean ridge axes, locations of which were obtained from global plate tectonic models (Figure 1) [*Minster and Jordan*, 1978; *DeMets et al.*, 1990].

2. Hydrothermal effluents achieve neutral buoyancy 300 m above the ridge axis, as has been observed over the Juan de Fuca Ridge [*Baker and Hammond*, 1992]. The hydrothermal plume is assumed to be 200 m wide vertically, with a central concentration maximum decaying linearly to zero symmetrically about the maximum. Because ridges range from 0 to 4000 m in depth, the injected ^{3}He at any given location is apportioned between the appropriate depth levels of the model. (Actual ridge axis depths, rather than smoothed model bathymetry, were used to determine the depth of introduction.)

3. The magnitude of ^{3}He injection is linearly proportional to the spreading rate, as tabulated by *DeMets et al.* [1990] and *Minster and Jordan* [1978]. A total ^{3}He flux of 1000 mol/yr is assumed, as is a ^{3}He/^{4}He ratio of about 10^{-5} (8 R_{air}), equivalent to a δ^3He value of 700%. This helium isotopic ratio is characteristic of ridge basalts and hydrothermal vents above ridges [e.g., *Lupton and Craig*, 1975; *Kurz et al.*, 1982].

4. The mantle helium component is superimposed on a uniform oceanic background distribution with Δ^4He values of 5% (relative to saturation at 3.8° C).

The GCM was iterated until an approximately steady-state He distribution was obtained. A steady-state He distribution is defined as an absence of flux imbalances greater than 10^{-8} kmol ^{3}He/yr.

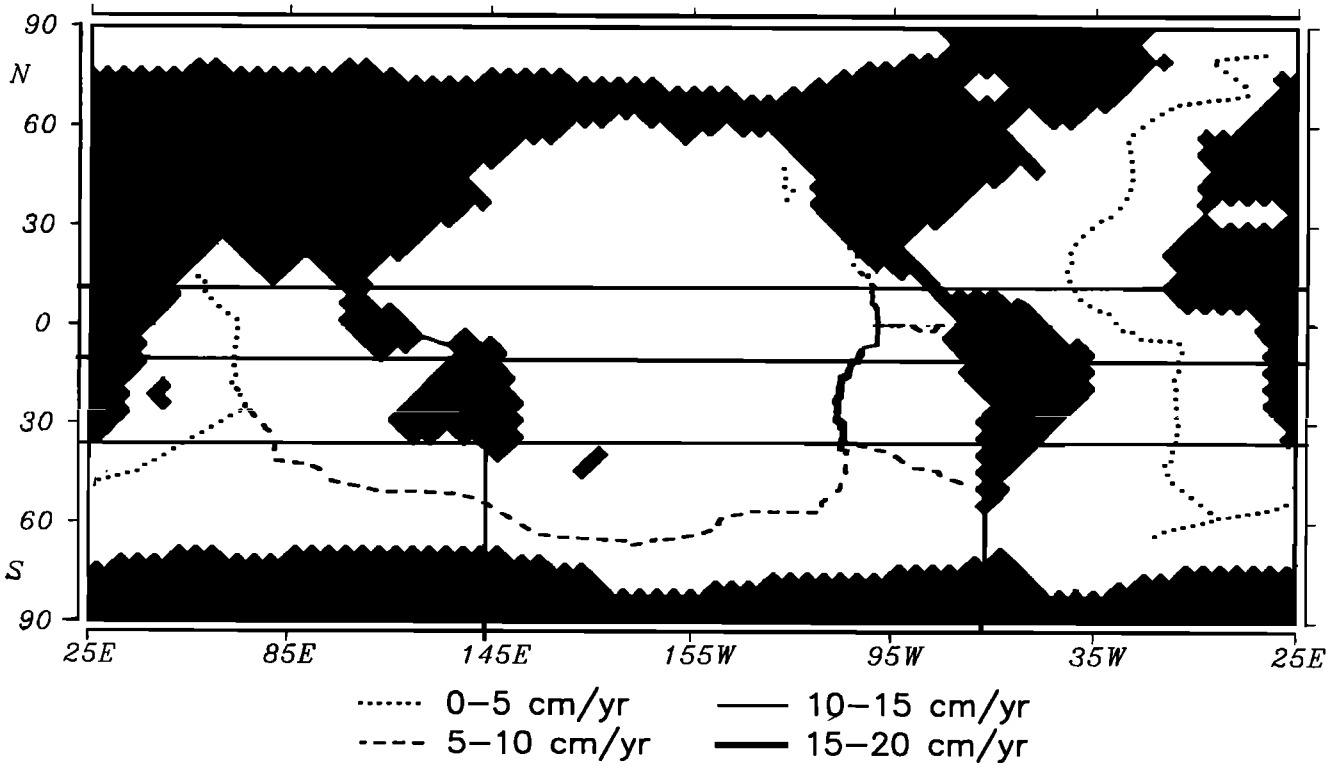

Figure 1. The distribution of mid-ocean ridges. The line style indicates the local full spreading rate. Grid lines indicate the boundaries between the subbasins used in Figure 2. The boundary between Atlantic and Indian basins occurs at 25°E.

Results and Discussion

In the following discussion we have subdivided the oceans into major basins (Pacific, Atlantic, Indian, Antarctic) and sub-basins (northern, tropical, southern, Antarctic) using the boundaries shown in Figure 1.

Mass Balances, Inventories, and Mean Residence Times

The simulated steady-state distribution and flux balance of helium within the ocean basins is shown in Figure 2. As a consequence of both spreading rate and mid-ocean ridge distribution, the simulated flux is spatially heterogeneous. Ridge fluxes into the Pacific, Atlantic, Indian, and Southern Oceans comprise respectively 31.5%, 13.9% , 10.5%, and 44% of the total. The GCM yields a steady-state mantle ^{3}He inventory of 978 kmol (51% residing in the Pacific, 9.3% in the Atlantic, 11% in the Indian, and 27% in the Antarctic). The total ^{3}He inventory (mantle + atmospheric) is about 4200 kmol [*Craig and Lupton,* 1981], so 23% of oceanic ^{3}He is directly derived from the mantle. Mantle helium has an apparent residence time of roughly 1000 years. As expected for a conservative gas tracer, this period is comparable to the mean turnover time of the oceans.

Figure 3 shows that loss of helium to the atmosphere occurs primarily in circumpolar (47% of the total) and tropical (27%) waters, reflecting regions of deep-water ventilation. The outgassing is largest from the Pacific and the Pacific sector of the Antarctic ocean. The imbalance between mantle input and ventilation leads to an annual export of ~100 mole of ^{3}He from the Pacific to the Atlantic sector of the Southern ocean via Drake Passage. Atmospheric losses and mantle input are approximately balanced in the Indian Ocean.

Differences in mantle He fluxes and ventilation rates of the individual ocean basins lead to large variations in the magnitude of the ^{3}He anomaly in each basin (Figure 2). The average δ^3He values are 13.4%, 3.4%, 12.6%, and 9.6% in the Pacific, Atlantic, Indian, and Antarctic seas, respectively. These are quite similar to measurement-based estimates [*Craig et al.*, 1975].

General Features and Comparison With Measurements

Pacific Ocean. The dominant feature of the simulated ^{3}He distribution in the Pacific Ocean is an intense maximum located at 2000-m depth over the EPR crest (Figures 4 and 5). This lobate feature is centered slightly south of the equator and reaches a maximum δ^3He value of 38%. It can be traced westward across the entire Pacific Basin as it shoals, dissipates, and narrows (Figures 4c and 5b). Northward and southward of the equator the helium anomalies diminish monotonically, reaching their lowest values by a rapid drop at the polar front, to δ^3He values of 8-10% in circumpolar waters.

This structure is produced by a combination of tectonic and oceanographic processes. The fastest EPR spreading and the largest helium flux occurs between the equator and 30°S. In addition, strong equatorial upwelling (inferred from simulated velocity profiles) tends to draw helium-rich deep waters toward

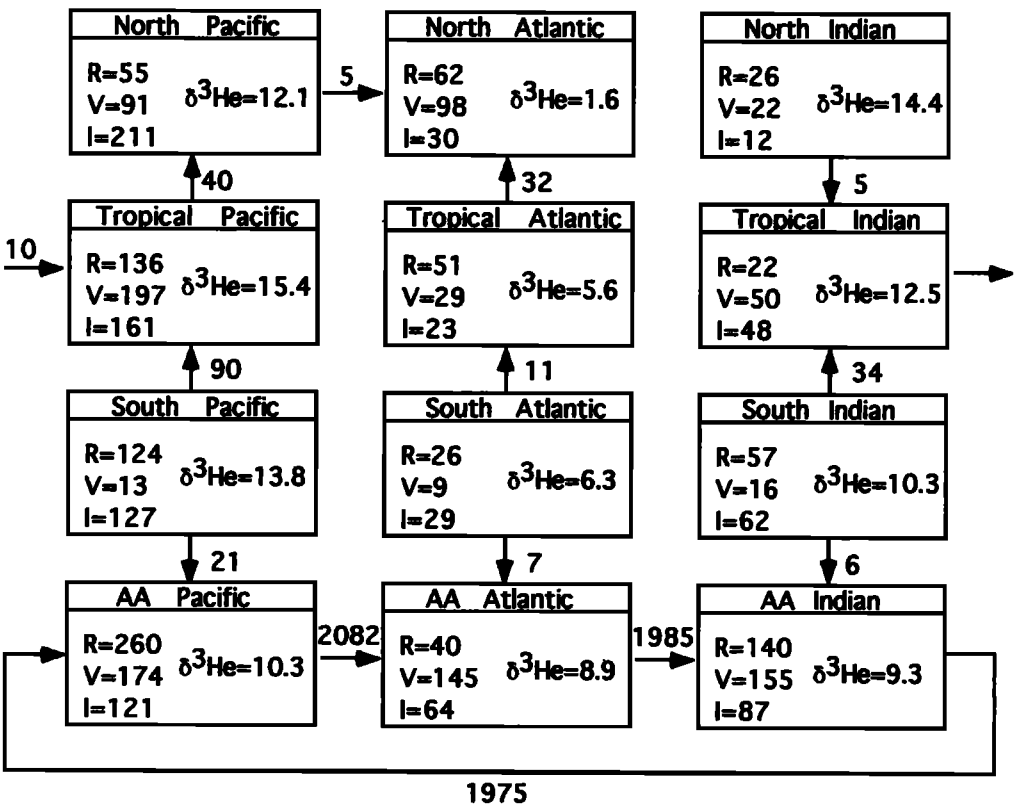

Figure 2. Basinal helium fluxes and modeled helium distribution for the basins indicated in Figure 1. *R* is the ridge flux and *V* the ventilation flux, in moles ^{3}He/year. Arrows indicate interbasinal fluxes, again in moles ^{3}He/year. I is the inventory of ^{3}He in each basin, in kilomoles. The basin-wide average δ^3He (percent) value is indicated.

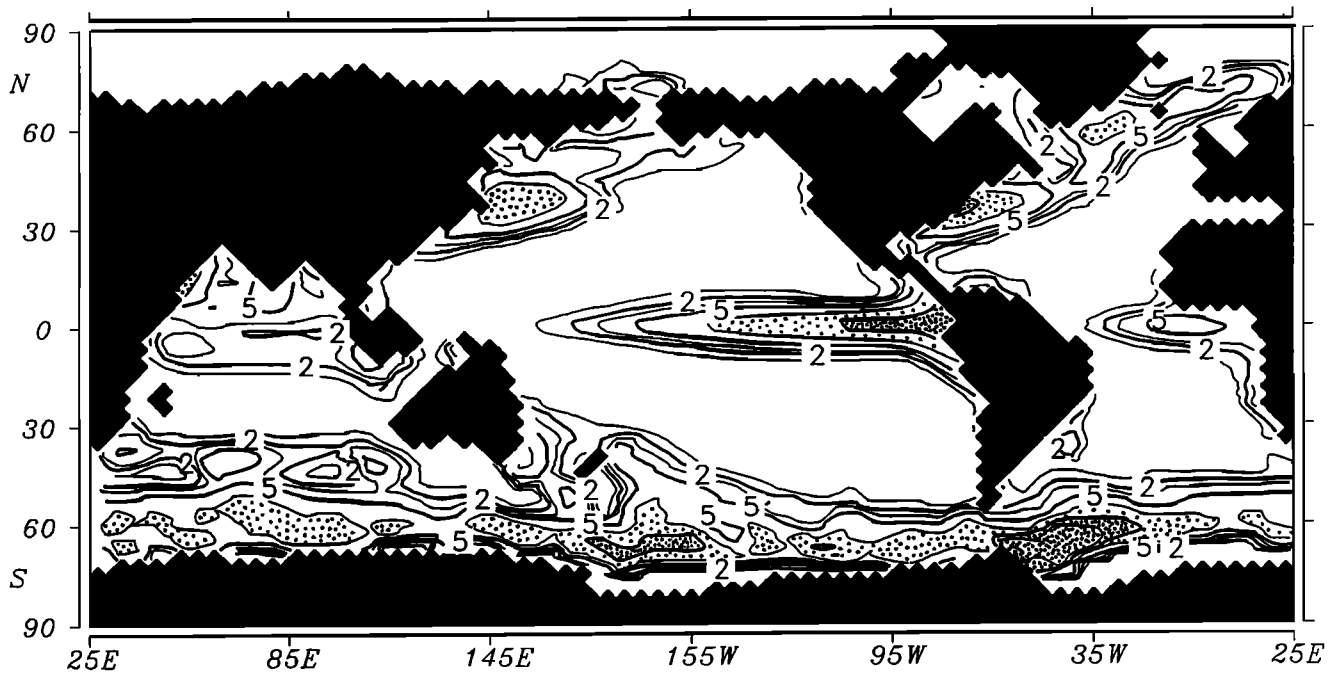

Figure 3. Annual outflux of mantle ^{3}He from the ocean surface, in picomoles per square meter. Contours are 1, 2, 3, 5, 10 and 20. Regions between 10 and 20 are lightly stippled, and >20, heavily stippled.

the equator and upward in the water column. This explains the westward shoaling, dissipation, and narrowing of the δ^3He maximum. An important consequence of this upwelling is extensive release of mantle helium to the atmosphere from Pacific equatorial waters (Figure 3).

In the circumpolar region, δ^3He is generally lower than it is elsewhere in the Pacific and is essentially invariant with depth below 1 km (Figure 4). These lower values are produced by ventilation and vertical mixing and by the introduction of relatively helium-poor Atlantic and Indian Ocean waters in the Antarctic Circumpolar Current (ACC). In the eastern margin of the circumpolar Pacific, the injection of He-rich waters originating in the mid-latitudes of the eastern Pacific is evidenced by a rapid increase in δ^3He from 10% to 14% (Figure 5c).

Several measured ^{3}He sections are available for comparison with these results; the most complete are the two N-S Geochemical Ocean Sections Study (GEOSECS) lines [*Ostlund et al.*, 1987]. The western Pacific GEOSECS line is reproduced in Figure 4d and is directly comparable to Figure 4c. The near-ridge (eastern) GEOSECS section (not shown) is characterized by a large high-δ^3He core at 2500-m depth roughly centered at the equator. The maximum measured anomaly (35%) is in excellent agreement with the simulated maximum (38%), confirming that the helium source function has been quantified reasonably well. Thus we believe that the estimated total mantle ^{3}He flux (4 atoms/cm^2/s [*Craig et al.*, 1975]) is approximately correct, as a fortuitous combination of errors in the flux and circulation would be required to produce this agreement otherwise.

The structure of the measured He maximum is also similar to that of the model: δ^3He values drop to about 20% at 35°S and to 10% in circumpolar waters. The simulated and observed maxima are of comparable vertical extent, and although the measured maximum is 500 m deeper than predicted by the model, this difference is insignificant given the vertical resolution of the GCM.

On the regional scale there are important differences between the simulated ^{3}He distribution and the GEOSECS results. Most noticeably, the GCM does not reproduce the two prominent "plume jets" located at 2500-m depth at 20°S and 5°N in the two GEOSECS sections (*Craig* [1990] and Figure 4d). Instead the GCM predicts a single, equatorially centered maximum across the entire Pacific Basin. The origin of the plume jets is unknown, but they apparently result from processes which have been ignored in the present model. Logical candidates are geothermal heating [*Stommel*, 1982] or physical processes which are on too fine a spatial scale for this model to reproduce. Alternatively, they may result from transient phenomena, such as intense recent volcanism and magma degassing.

Regardless of the origin of the plume jets, the difference between the model simulation and the GEOSECS data is useful for interpreting the GCM results. Unlike the model maximum, which shoals, narrows, and dissipates to the west, the observed ^{3}He maxima remain at the same depth, latitude, and approximate intensity across the entire Pacific. This difference demonstrates that upwelling and lateral diffusivity are both overly-intense in the GCM, because even if such jets were produced by some (transient?) mechanism on the EPR, the model flow field would cause them to coalesce and upwell at the equator. The stronger upward transport of ^{3}He in the model compared with observations is in agreement with anomalously shallow isotherms near the equator (not shown). This effect has been noticed previously and is a consequence of the coarse resolution of this GCM [*Maier-Reimer*, 1993].

Indian Ocean. The simulated helium distribution in the Indian Ocean is very different from that in the Pacific. Rather than a single maximum overlying the spreading center, the model predicts a large mid-depth water mass with high δ^3He values (up to 16%) originating in the Gulf of Aden (Figure 6). Southward

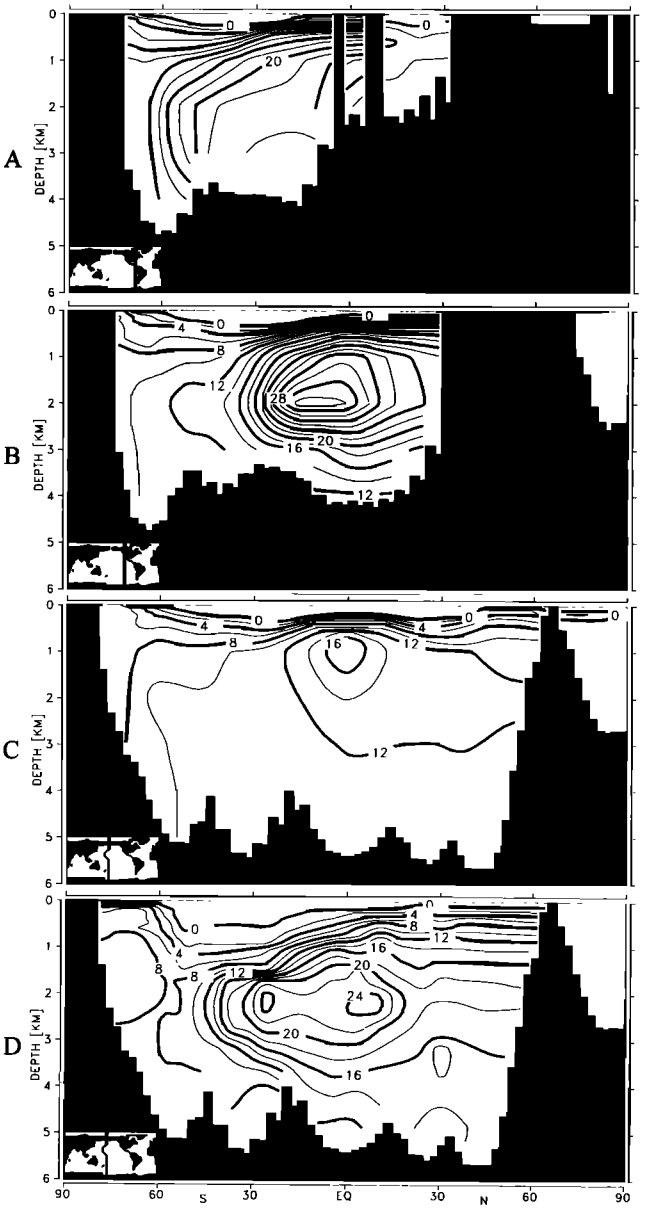

Figure 4. North-South δ^3He (percent) sections across the Pacific Ocean. The location of each section is indicated in the map at the lower left corner of each figure. Figures 4a, 4b, and 4c show the results from the GCM. Figure 4d shows the western Pacific Geochemical Ocean Sections Study (GEOSECS) helium data [*Ostlund et al.*, 1987]. Note that Figure 4c lies along the western Pacific GEOSECS track.

and to the east and west of the Arabian Sea, δ^3He values drop steadily, to about 9% in the subpolar waters. In general there is little structure to the δ^3He distribution with depth. The only exception to this observation is in the eastern Indian Basin, where there is a noticeable mid-depth maximum induced by northward penetration of recently ventilated (helium-poor) bottom waters. This penetration does not extend into the western portion of the basin. In the western circumpolar region the influx of ^{3}He-rich ACC waters is discernible as a local maximum (Figures 3 and 4d). Ventilation of the ACC is indicated by the steady eastward decrease in δ^3He across the Indian Ocean sector (Figure 5).

The absence of intense, well-defined ^{3}He maxima in the model Indian Ocean is likely the result of fairly slow spreading rates (typically 20% of Pacific rates). Unlike the Pacific, upwelling is relatively weak, and there is no tendency for ^{3}He-rich waters to coalesce at the equator.

Measured deep-water ^{3}He sections across the Indian Ocean are available from GEOSECS (Figure 6d) and from *Jamous et al.* [1992]. These reveal a broad tongue of high δ^3He water extending southward from the Gulf of Aden at 2500-m depth. Helium anomalies decay from a high of about 16% at the northern margin of the Indian Basin to around 8% at 50°S. At 55°-60°S a well-developed core of helium-rich water (δ^3He=10%) enters at around 1000-m depth, dissipating gradually to the east.

These observed features are in excellent agreement with the model; both the general structure and the absolute magnitude of the ^{3}He anomalies are reproduced. The only significant

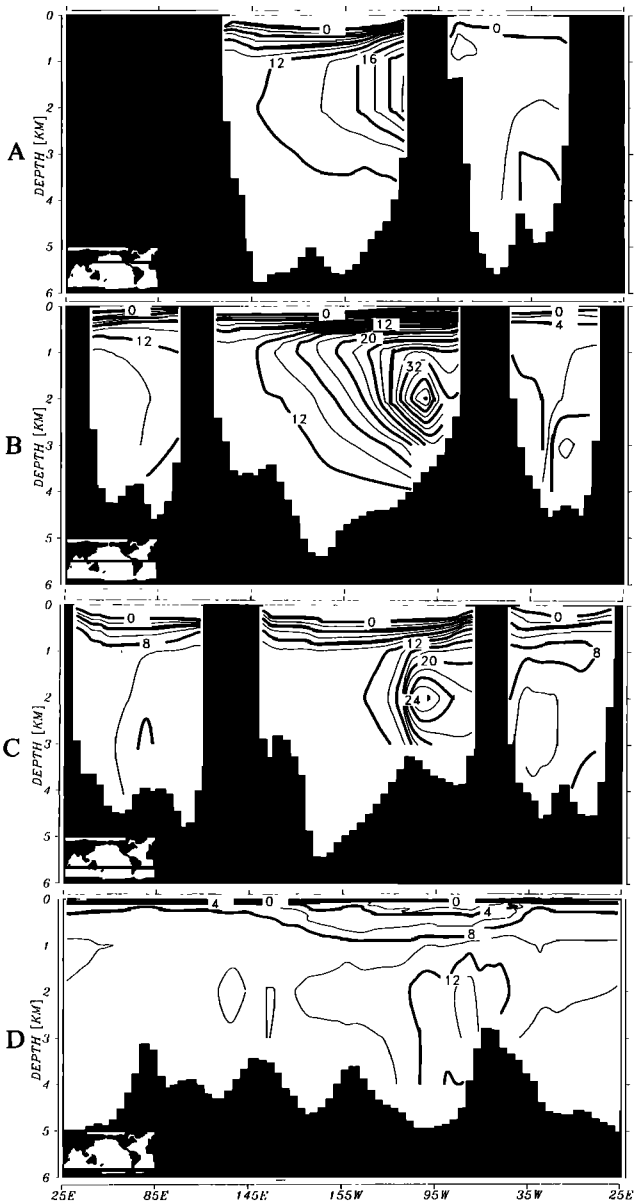

Figure 5. Simulated east-west δ^3He (percent) sections at (a) 30°N, (b) 0°, (c) 30°S, and (d) 60°S.

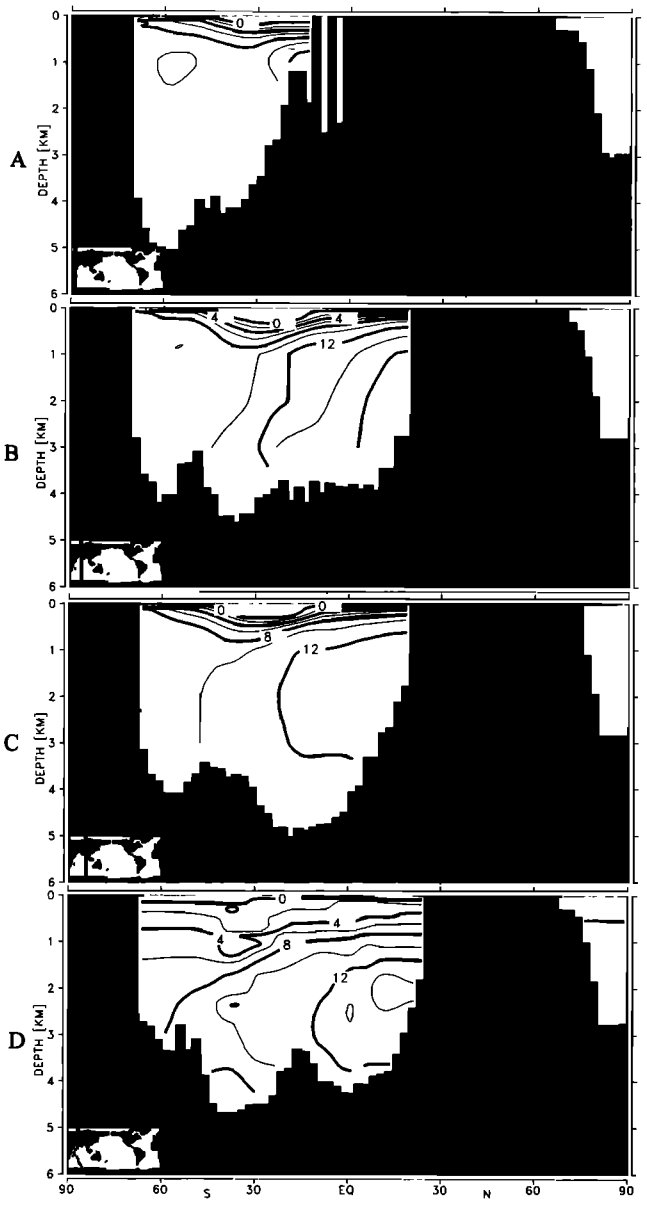

Figure 6. North-South δ^3He (percent) sections across the Indian Ocean. The location of each section is indicated in the map at the lower left corner of each figure. Panels A-C show the results from the GCM. Panel D shows the GEOSECS helium data [*Ostlund et al.*, 1987] and is roughly comparable to Panel B.

discrepancy is that the model does not reproduce the strong penetration of ventilated bottom waters observed in the western Indian Ocean (e.g., Figure 6c). These bottom waters are formed mainly in the Weddell Sea and possibly also on the Antarctic continental slope in the Indian sector of the Southern Ocean.

An additional discrepancy exists in the northeastern part of the Indian basin, where the introduction of ^{3}He-rich Pacific waters through the Indonesian Passage has been observed [*Jamous et al.*, 1992]. Because the model forces intense ventilation of Pacific equatorial waters, the simulated ^{3}He concentrations in the western Pacific are relatively low compared with observations. As a consequence, injection of western Pacific waters does not produce a local ^{3}He maximum in the simulated Indian Ocean ^{3}He distribution.

Atlantic Ocean. The smallest simulated δ^3He values occur in the Atlantic Ocean, where seafloor spreading is slowest and ventilation is fastest. The penetration of recently ventilated North Atlantic Deep Water (NADW) between helium-rich Antarctic Bottom Water (AABW) and Antarctic Intermediate Water (AAIW) leads to a simulated ^{3}He minimum centered around 2500-m depth throughout the basin (Figures 4, 5, and 7). During its southward migration, the NADW becomes increasingly enriched in ^{3}He, rising from nearly the solubility equilibrium value (-1.8%) at high northern latitudes to as high as 8% at about 45°S. This increase is a result of continuous integration of the ^{3}He injected from the MAR supplemented by mixing with the overlying and underlying ^{3}He-rich water masses. At 50°-60°S a core of circumpolar water with a δ^3He value of about 12% crosses the Atlantic at 2000-m depth. In agreement with Figure 2, this clearly demonstrates the influx of Pacific helium into the Atlantic Basin. As in the Indian Ocean, there is no evidence for intense ^{3}He maxima; strong δ^3He gradients are absent both in the vertical and horizontal dimensions.

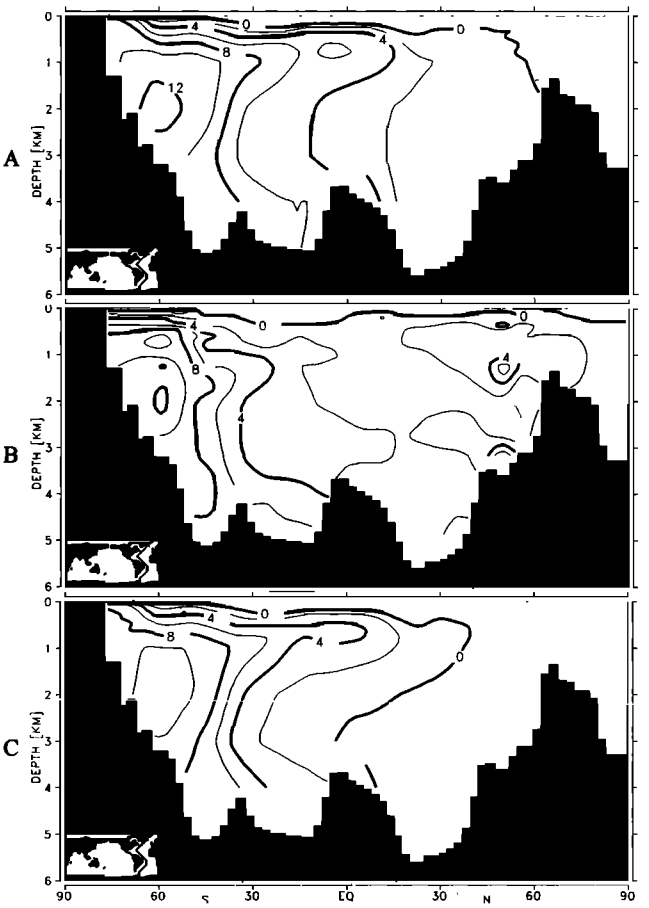

Figure 7. Sections of δ^3He (percent) along the Atlantic GEOSECS line. (a) GCM results using the standard source function. (b) GEOSECS helium data [*Ostlund et al.*, 1987]. (c) GCM output which results from assuming no injection of helium from the Mid-Atlantic Ridge. Note that the ^{3}He enrichments in the northern Atlantic GEOSECS data are the product of tritium decay.

The western Atlantic GEOSECS section (Figure 7b) is useful for a comparison with the simulation. Ignoring the intrusion of tritiogenic helium in the North Atlantic, the measurements define the same features as the model: a core of ^{3}He-poor NADW lying between the two high δ^3He Antarctic water masses (AAIW, AABW). A steady southward increase in the deep-water δ^3He is abruptly accelerated at 60°S, where this section intersects the ACC. Their similar structure notwithstanding, there is a major difference in the absolute magnitude of the simulated and measured δ^3He fields. While the predicted circumpolar δ^3He value of 12% is indistinguishable from the GEOSECS data, the simulated NADW has uniformly higher δ^3He than is actually observed. For example, at 30°S and 3000-m depth, the model predicts a δ^3He value of nearly 6%, but the measured value is only 3%. Discrepancies of a similar magnitude exist throughout the Atlantic Basin. Previous workers [*Lupton*, 1976; *Broecker*, 1980] have also noted the apparent deficiency of ^{3}He in the Atlantic.

The excessively high δ^3He in model NADW is puzzling, particularly because the GCM does a good job simulating the transient tracers in this water mass [*Maier-Reimer*, 1993]. Because the GCM grossly reproduces the magnitude and distribution of ^{3}He anomalies elsewhere in the oceans, it seems unlikely that this discrepancy can be attributed to an overestimation of the global source strength. Nor can it be attributed to the absence of tritiogenic helium in the GCM, because this would cause the simulated δ^3He values to be lower than observed values, rather than higher. Lower than simulated Atlantic δ^3He values must result either from an unexpected injection of ^{4}He (which would lower the helium isotopic ratio), or from smaller than expected injection of ^{3}He into the Atlantic Basin.

Broecker [1980] suggested that influx of a low ^{3}He/^{4}He component may mask the effects of ridge helium injection in the Atlantic. If so, the ^{4}He source would have to be large and injected uniformly into NADW. An anomalously large air component (δ^3He=0) can be eliminated because the degree of helium supersaturation required is excessive. To lower δ^3He from a predicted value of 6% to the observed 3% would raise the helium concentration to more than twice the saturation value. Such supersaturation is physically unreasonable and in any case is not supported by helium concentration measurements [e.g., *Jenkins and Clarke*, 1976].

Injection of radiogenic helium (nearly pure ^{4}He) has been inferred in several restricted oceanic basins [*Top et al.*, 1980; *Top and Clarke*, 1983] and could conceivably occur in the open Atlantic. The increase in helium concentration necessary to lower δ^3He sufficiently is about 3% and would probably not be detectable given the natural variability in the degree of oceanic helium supersaturation. Is the magnitude of the required flux reasonable? If the reduction occurs in a 3-km-thick water column (typical NADW thickness) and is generated in 200 years (about the time for NADW to migrate from its formation region to 30°S), an average flux of 1.6×10^6 atoms ^{4}He/cm^2/s is required. This estimate is of the same order of magnitude as has been suggested for Baffin Bay [*Top et al.*, 1980]. However such a large flux cannot be attributed solely to steady-state radioactive decay in the sediments. Using average sediment compositions of 1.5 ppm U, a Th/U ratio of 5 [*Ben Othman et al.*, 1989] and a column-averaged sediment density of 2000 kg/m^3, support of this flux would require a sediment pile 24 km thick. This is far larger than actually exists throughout the Atlantic Basin. Thus for this explanation to be viable, it is necessary to postulate loss of helium from very old mineral grains within the sediment. This mechanism is difficult to evaluate quantitatively, but seems unreasonably contrived.

A plot of δ^3He against phosphate corrected for biological effects, PO_4^* [*Maier-Reimer*, 1993], provides additional insights to the origin of this discrepancy. Like ^{3}He, PO_4^* is a conservative tracer that has high values in the circumpolar regions and low values in young NADW (Figure 8). In the absence of a mantle helium flux, these two tracers would be linearly correlated in NADW. However, because the simulated NADW experiences injection of mantle helium, a strong curvature toward higher δ^3He values is predicted (Figure 8). This curvature demonstrates the importance of MAR helium input to the simulated Atlantic. In contrast, ^{3}He and PO_4^* measurements from the western Atlantic GEOSECS section covary nearly linearly (Figure 8). The GEOSECS data thus seem to preclude large-scale injection of mantle ^{3}He into the Atlantic.

To explore the possibility that the Atlantic helium flux is much smaller than we have estimated, we have rerun the GCM under the limiting assumption that there is no mantle helium injected at the MAR. As is shown in Figure 7c, this modification yields a helium distribution in much better agreement with observations. For example, the δ^3He value at 30°S and 3000 m depth drops from 6% to the observed value of 3%. In addition, the bulge in the δ^3He-PO_4^* relationship disappears, making the simulated and observed arrays nearly indistinguishable (Figure 8). Because the Atlantic contributes very little helium to the other oceans, eliminating the MAR helium flux does not substantially alter the He distribution outside of the Atlantic basin.

A further test comes from independent estimates of the flux of mantle helium into the Greenland-Norwegian-Eurasian Basins. From the observed water column inventory of ^{3}He, *Schlosser et al.* [1991b] have estimated a flux of roughly 1.6 mol ^{3}He/yr. Using our estimate of the flux per unit of spreading and the length (~3300 km) and average spreading rate (~1 cm/yr [*DeMets et al.*, 1990]) of these basins yields an estimate of nearly 11 mol ^{3}He/yr. This confirms a much lower than anticipated flux into the polar Atlantic.

Unlike the Pacific and most of the Indian ridge segments, the MAR axis is situated at the bottom of a rift valley up to 1 km deep. Retention of hydrothermal effluents within the axial valleys has been offered to account for the relatively low abundances of hydrothermal Mn in the open Atlantic [*Klinkhammer et al.*, 1985] and could potentially affect the helium distribution. However, rift valleys cannot be a permanent sink for helium, which must ultimately be released into the overlying water column (the same is not true for Mn, a highly nonconservative species). Therefore we must postulate that the present-day He flux from the mantle to the Atlantic basin is smaller than our simple source function predicts. This lower flux is probably not a consequence of systemtaically lower-than-average He concentrations in Atlantic ridge lavas, because the most He-rich known basalts actually occur on the MAR [*Staudacher et al.*, 1989].

The most distinctive feature of the MAR relative to the rest of the global ridge system is its very low spreading rates. Although the assumption of a linear correlation between helium flux and spreading rate is intuitively reasonable, the Atlantic GCM results may indicate that this assumption does not hold on the slowest ridge segments. This could result either from

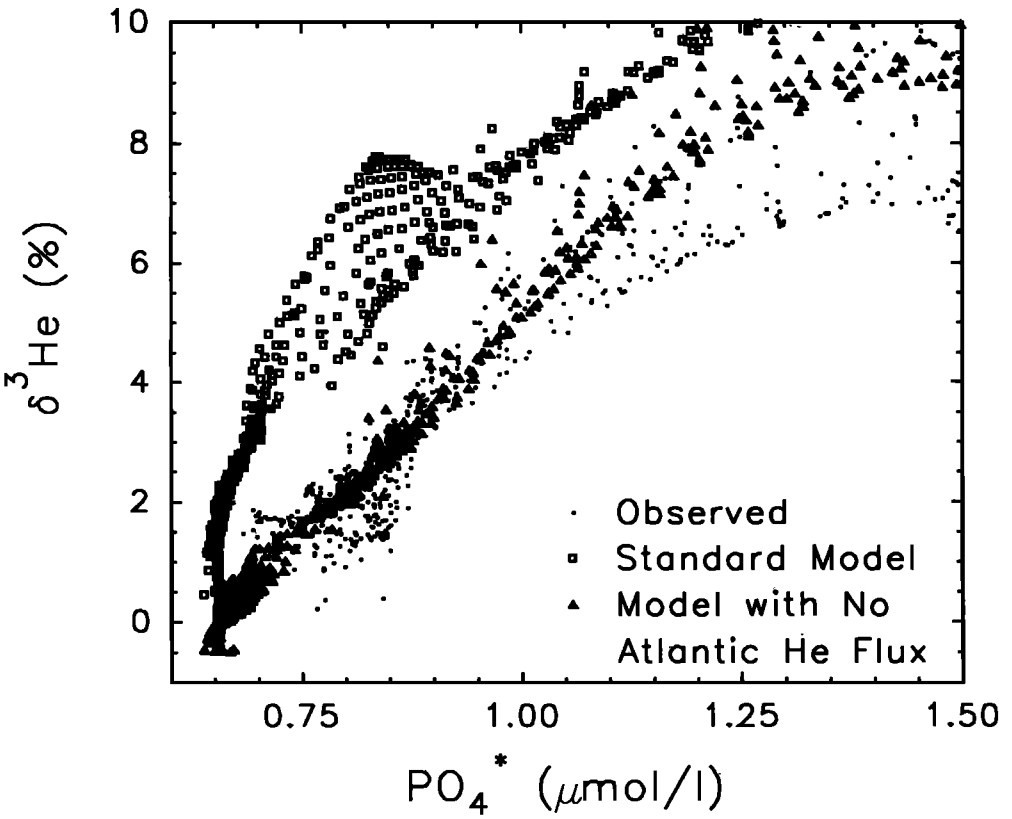

Figure 8. Plot of δ^3He versus phosphate corrected for biological effects, PO_4^*, for the Atlantic below 1000-m depth and north of 50°S. The observed results are interpolated into the GCM grid from GEOSECS measurements. The GCM output using both the standard helium source and a source which assumes no helium injection from the MAR are indicated.

variations in crustal thickness or from the process that releases mantle helium to the seafloor.

We have assumed that oceanic crustal thicknesses and consequently the amount of magma emplaced on the seafloor per unit of seafloor spreading are constant. This assumption is well supported at moderate to fast spreading rates, but there is a dramatic decrease in crustal thickness when spreading rates drop below 2 cm/yr [*Bown and White,* 1994]. While this may lead to somewhat smaller fluxes of He into portions of the far northern Atlantic, most of the MAR spreads substantially faster than this critical value. It is also possible that the absence of a magma chamber on most of the MAR (in contrast to the faster spreading ridges [*Sinton and Detrick,* 1992]) may somehow impede the crustal degassing process. Additional studies of a variety of well-characterized ridge segments are required to evaluate how the helium flux varies with spreading rate.

An alternative explanation is that our assumption of steady-state injection becomes invalid at slow spreading rates. If hydrothermal venting is of short duration following eruptions and the eruptions are highly episodic, then the present ^{3}He-poor state of the Atlantic may record a period of extended quiescence (~200 years) during which no major eruptions have occurred on the MAR. If so, then the estimated flux of 1000 mol ^{3}He/year is an instantaneous value which may not be representative of the average flux. Our present understanding of both eruption periodicity and hydrothermal vent longevity are too poor to evaluate this possibility.

Conclusions

This first attempt to couple an oceanic GCM with estimates of the hydrothermal helium flux from the mantle yields average δ^3He values and interbasin gradients which are in good agreement with observations. The gross distribution of ^{3}He within individual ocean basins is also reproduced reasonably well. The agreement between simulated and measured ^{3}He fields indicates that mantle helium sources other than mid-ocean ridges (e.g., hotspots, convergent margins) are not important in models of this resolution and that a total mantle ^{3}He flux of 1000 mol/yr is approximately correct. For the Indian and Pacific Oceans, our assumption of a linear relationship between seafloor spreading rate and mantle helium flux appears to be appropriate. However, discordance between the simulated and measured ^{3}He field in the Atlantic Ocean requires either a very sharp dropoff in helium flux at slow spreading rates (< 3 cm/yr), a very large flux of radiogenic helium from the seafloor, or episodic injection. Further studies of the helium flux from sediments and from ridges spreading at a variety of rates are necessary to resolve this issue.

Despite these complications, the accuracy of deep-water circulation predicted by the GCM can be evaluated. The general agreement between simulated and measured ^{3}He abundances and distributions supports the large-scale flow field and ventilation rates in the GCM. However, there are noticeable deviations on the regional scale. For example, it is particularly

apparent that lateral diffusivity and equatorial upwelling (down to depths of several kilometers) are too intense in the GCM, especially in the Pacific. There is also an indication that insufficient bottom water is injected into portions of the western Indian Ocean.

Acknowledgements. We thank Keith Dixon for a thorough and constructive review of this manuscript. This work was supported by NSF Grant OCE-9111404 (P.S.). This is LDEO contribution number 5293.

References

Baker, E., and S. R. Hammond, Hydrothermal venting and the apparent magmatic budget of the Juan de Fuca Ridge, *J. Geophys. Res., 97*, 3443-3456, 1992.

Belviso, S., P. Jean-Baptiste, B. C. Nguyen, L. Merlivat, and L. Labeyrie, Deep methane maxima and ^{3}He anomalies across the Pacific entrance to Celebes Basin, *Geochim. Cosmochim. Acta, 51*, 2673-2680, 1987.

Ben Othman, D., W.M. White, and J. Patchett, The geochemistry of marine sediments, island are magmagenesis and crust-mantle recycling, *Earth Planet. Sci. Lett., 94*, 1-21, 1989.

Benson, B. B., and D. Krause, Isotopic fractionation of helium during solution: A probe for the liquid state, *J. Solution Chem., 9*, 895-909, 1980.

Bown, J. W., and R. S. White, Variation with spreading rate of crustal thickness and geochemistry, *Earth Planet. Sci. Lett., 121*, 435-450, 1994.

Broecker, W. S., The distribution of ^{3}He anomalies in the deep Atlantic, *Earth Planet. Sci. Lett., 49*, 513-519, 1980.

Broecker, W. S., T. H. Peng, G. Ostlund, and M. Stuiver, The distribution of bomb radiocarbon in the ocean, *J. Geophys. Res., 90*, 6953-6970, 1985.

Clarke, W. B., M. A. Beg, and H. Craig, Excess He-3 in the sea: Evidence for terrestrial primordial helium, *Earth Planet. Sci. Lett., 6*, 213-221, 1969.

Craig, H., The HELIOS helium-3 jets in the North and South Pacific, *Eos Trans AGU, 71*, 1396, 1990.

Craig, H., and J. E. Lupton, Helium-3 and mantle volatiles in the ocean and the oceanic crust, in *The Sea*, vol. 7, *The Oceanic Lithosphere*, edited by C. Emiliani, pp. 391-428. Wiley Interscience, New York, 1981.

Craig, H., and R. F. Weiss, Dissolved gas saturation anomalies and excess helium in the ocean, *Earth Planet. Sci. Lett., 10*, 289-296, 1971.

Craig, H., W.B. Clarke, and M.A. Beg, Excess ^{3}He in deep water on the East Pacific Rise, *Earth Planet. Sci. Lett., 26*, 125-132, 1975.

DeMets, C., R. G. Gordon, D. F. Arsus, and S. Stein, Current plate motions, *Geophys J. Int., 101*, 425-478, 1990.

Dymond, J. and L. Hogan, Factors controlling the noble gas abundance patterns of deep sea basalts, *Earth Planet. Sci. Lett., 38*, 117-128, 1978.

Fiadero M. E., Three-dimensional modeling of tracers in the deep Pacific Ocean, II, Radiocarbon and the circulation, *J. Mar. Res., 50*, 537-550, 1982.

Gamo, T., J.-I. Ishibashi, H. Sakai, and B. Tilbrook, Methane anomalies in seawater above the Loihi submarine summit area, Hawaii, *Geochim. Cosmochim. Acta, 51*, 2857-2864, 1987.

Jamous, D., L. Memery, C. Andrié, P. Jean-Baptiste, and L. Merlivat, The distribution of helium 3 in the deep western and southern Indian Ocean, *J. Geophys. Res., 97*, 2243-2250, 1992.

Jean-Baptiste, P., S. Belviso, G. Alaux, B. C. Nguyen and N. Mihalopoulos, ^{3}He and methane in the Gulf of Aden, *Geochim. Cosmochim. Acta, 54*, 111-116, 1990.

Jenkins, W. J., and W. B. Clarke, The distribution of ^{3}He in the western Atlantic Ocean, *Deep Sea Res., 23*, 481-494, 1976.

Jenkins, W., P. A. Rona and J. M. Edmond, Excess ^{3}He in the deep water over the Mid-Atlantic Ridge at 26° N: Evidence of hydrothermal activity, *Earth Planet. Sci. Lett., 49*, 39-44, 1980.

Kellogg, L., and J.G. Wasserburg, The role of plumes in mantle helium fluxes, *Earth Planet. Sci. Lett., 99*, 276-289, 1990.

Klinkhammer, G., P. Rona, M. Greaves, and H. Elderfield, Hydrothermal manganese plumes in the Mid-Atlantic Ridge rift valley, *Nature, 314*, 727-731, 1985.

Kurz M. D., W. J. Jenkins, J.-G. Schilling, and S. R. Hart, Helium isotopic variations in the mantle beneath the central North Atlantic Ocean, *Earth Planet. Sci. Lett., 58*, 1-14, 1982.

Lupton, J. E., The He-3 distribution in deep water over the Mid-Atlantic Ridge, *Earth Planet. Sci. Lett., 32*, 371-374, 1976.

Lupton, J. E., and H. Craig, Excess He-3 in oceanic basalts: Evidence for terrestrial primordial helium, *Earth Planet. Sci. Lett., 26*, 133-139, 1975.

Lupton, J. E., and H. Craig, A major ^{3}He source at 15°S on the East Pacific Rise, *Science, 214*, 13-18, 1981.

Lupton, J. E., J. R. Delaney, H. P. Johnson, and M. K. Tivey, Entrainment and vertical transport of deep-ocean water by buoyant hydrothermal plumes, *Nature, 316*, 621-623, 1985.

Lupton J. E., E. T. Baker, and G. J. Massoth, Variable ^{3}He/heat ratios in submarine hydrothermal systems: Evidence from two plumes over the Juan de Fuca Ridge, *Nature, 337*, 161-164, 1989.

Maier-Reimer, E., Geochemical cycles in an ocean general circulation model: Preindustrial tracer distributions, *Global Biogeochem. Cycles, 7*, 645-677, 1993.

Maier-Reimer, E., U. Mikolajewicz, and K. Hasselmann, Mean circulation of the Hamburg LSG OGCM and its sensitivity to the thermohaline surface forcing, *J. Phys. Oceanogr., 23*, 731-757, 1993.

Minster, J. B., and T. H. Jordan, Present day plate motions, *J. Geophys. Res., 83*, 5301-5354, 1978.

Ostlund, H. G., H. Craig, W. S. Broecker, and D. Spencer (Eds.), GEOSECS *Atlantic, Pacific and Indian Ocean Expeditions; Shorebased Data and Graphics*, vol. 7, 230 p., National Science Foundation, Washington, D.C., 1987.

Parsons, B., The rates of plate construction and consumption, *Geophys J.R. Astron. Soc., 67*, 437-448, 1981.

Roether, W., P. Schlosser, R. Kuntz and W. Weiss, Transient-tracer studies of the thermohaline circulation of the Mediterranean, in *Winds and Currents of the Mediterranean Basin, 41*, vol. 2, edited by H. Charnock, pp. 291–317, 1992.

Sarmiento, J. L., and J. Bryan, An ocean transport model for the North Atlantic, *J. Geophys. Res., 87*, 394-408, 1982.

Schlosser, P., Helium: A new tracer in Antarctic oceanography, *Nature, 321*, 233-235, 1986.

Schlosser, P., E. Suess, R. Bayer, and M. Rhein, ^{3}He in the Bransfield Strait: Indication of local injection from back-arc rifting, *Deep Sea Res., 35*, 1919-1935, 1988.

Schlosser, P., J. L. Bullister, and R. Bayer, Studies of deep water formation and circulation in the Weddell Sea using natural and anthropogenic tracers, *Mar. Chem., 35*, 97-122, 1991a.

Schlosser, P., G. Bonisch, M. Rhein, and R. Bayer, Reduction of Greenland Sea Deep Water formation during the 1980's: Evidence from tracer data, *Science, 251*, 1054-1056, 1991b.

Sinton, J. M., and R. S. Detrick, Mid-ocean ridge magma chambers, *J. Geophys. Res., 97*, 197-216, 1992.

Staudacher T., P. Sarda, S.H. Richardson, C.J. Allegre, I. Sagna, and L.V. Dmitriev, Noble gases in basalt glasses from a Mid-Atlantic Ridge topographic high at 14°N: Geodynamic consequences, *Earth Planet. Sci. Lett., 96*, 119-133, 1989.

Stommel, H., Is the South Pacific helium-3 plume dynamically active?, *Earth Planet. Sci. Lett., 61*, 63-67, 1982.

Toggweiler, J. R., K. Dixon, and K. Bryan, Simulations of radiocarbon in a coarse-resolution world ocean model, 1, Steady-state prebomb distributions, *J. Geophys. Res., 94*, 8217-8242, 1989.

Top, Z., and W. B. Clarke, Helium, neon and tritium in the Black Sea, *J. Mar. Res., 41,* 1-17, 1983.

Top, Z., W. B. Clarke, W. C. Eismont, and E. P. Jones, Radiogenic helium in Baffin Bay bottom water, *J. Mar. Res., 38,* 435-453, 1980.

Top Z., W. B. Clarke, and W. J. Jenkins, Tritium and primordial ^{3}He in the North Atlantic: A study in the region of Charlie Gibbs Fracture Zone, *Deep Sea Res., 34,* 287-298, 1987.

Torgerson, T., Terrestrial helium degassing fluxes and the atmospheric helium budget: Implications with respect to the degassing processes of continental crust, *Chem. Geol., 79,* 1-14, 1989.

Weiss, R. F., J. L. Bullister, R. H. Gammon, and M. J. Warner, Chlorofluoromethanes in the upper North Atlantic Deep Water, *Nature, 314,* 608-610, 1985.

W.S. Broecker and P. Schlosser, Lamont-Doherty Earth Observatory of Columbia University, Palisades, NY 10964.

K.A. Farley, Division of Geological and Planetary Sciences, MC: 170-25, California Institute of Technology, Pasadena, CA 91125 (e-mail: farley@legs.gps.caltech.edu)

E. Maier-Reimer, Max-Planck-Institut für Meteorologie, Bundesstrasse 55, D-20146, Hamburg, Germany

(Received April 7, 1994; revised October 24, 1994;
accepted November 2, 1994.)